



Updating sea spray aerosol emissions in the Community Multiscale Air Quality (CMAQ) model version 5.0.2

B. Gantt^{1,2}, J. T. Kelly², and J. O. Bash¹

¹Atmospheric Modeling and Analysis Division, National Exposure Research Laboratory, Office of Research and Development, US Environmental Protection Agency, RTP, NC, USA

²Office of Air Quality Planning and Standards, US Environmental Protection Agency, Research Triangle Park, NC, USA

Correspondence to: J. O. Bash (bash.jesse@epa.gov)

Received: 7 April 2015 – Published in Geosci. Model Dev. Discuss.: 20 May 2015

Revised: 24 September 2015 – Accepted: 21 October 2015 – Published: 19 November 2015

Abstract. Sea spray aerosols (SSAs) impact the particle mass concentration and gas-particle partitioning in coastal environments, with implications for human and ecosystem health. Model evaluations of SSA emissions have mainly focused on the global scale, but regional-scale evaluations are also important due to the localized impact of SSAs on atmospheric chemistry near the coast. In this study, SSA emissions in the Community Multiscale Air Quality (CMAQ) model were updated to enhance the fine-mode size distribution, include sea surface temperature (SST) dependency, and reduce surf-enhanced emissions. Predictions from the updated CMAQ model and those of the previous release version, CMAQv5.0.2, were evaluated using several coastal and national observational data sets in the continental US. The updated emissions generally reduced model underestimates of sodium, chloride, and nitrate surface concentrations for coastal sites in the Bay Regional Atmospheric Chemistry Experiment (BRACE) near Tampa, Florida. Including SST dependency to the SSA emission parameterization led to increased sodium concentrations in the southeastern US and decreased concentrations along parts of the Pacific coast and northeastern US. The influence of sodium on the gas-particle partitioning of nitrate resulted in higher nitrate particle concentrations in many coastal urban areas due to increased condensation of nitric acid in the updated simulations, potentially affecting the predicted nitrogen deposition in sensitive ecosystems. Application of the updated SSA emissions to the California Research at the Nexus of Air Quality and Climate Change (CalNex) study period resulted in a modest improvement in the predicted surface concentration of sodium and nitrate at several central and southern California coastal sites.

This update of SSA emissions enabled a more realistic simulation of the atmospheric chemistry in coastal environments where marine air mixes with urban pollution.

1 Introduction

Sea spray aerosols (SSAs) contribute significantly to the global aerosol burden, both in terms of mass (Lewis and Schwartz, 2004) and cloud condensation nuclei concentration (Murphy et al., 1998; Pierce and Adams, 2006; Clarke et al., 2006; Blot et al., 2013). The chemical composition of SSAs (e.g., major ions: Na^+ , Mg^{2+} , Ca^{2+} , K^+ , Cl^- , SO_4^{2-} ; Tang et al., 1997) is affected by atmospheric processing, with the uptake of nitric acid (Gard et al., 1998, and references therein), sulfuric acid (McInnes et al., 1994), dicarboxylic acids (Sullivan and Prather, 2007), and methylsulfonic acid (Hopkins et al., 2008) shown to be important processes. Sea spray aerosols also influence gas-phase atmospheric chemistry via displacement of chlorine and bromine from the particle phase and subsequent impacts on ozone formation and destruction (Yang et al., 2005; Long et al., 2014). Despite this importance, much uncertainty remains in the factors affecting the size-dependent production flux per whitecap area, which drives the emission rates in most chemical transport models (de Leeuw et al., 2011).

An active area of recent research has been in the determination of the SSA size distribution. The size distribution of particles influences their atmospheric lifetime, surface area available for heterogeneous reactions, cloud condensation nuclei efficiency, and optical properties. A widely

used SSA emission parameterization in early chemical transport models was described by Monahan et al. (1986), which predicts the size distribution between 0.8 and 8 μm in dry diameter based on laboratory measurements. To address the overpredicted SSA emission rate when the parameterization from Monahan et al. (1986) was extended to aerosol dry diameters $< 0.2 \mu\text{m}$ (Andreas, 1998; Vignati et al., 2001), Gong (2003) revised the Monahan et al. (1986) parameterization to match the SSA size distribution observed in the North Atlantic (O'Dowd et al., 1997) down to a 0.07 μm dry diameter. Since the publication of Gong (2003), several studies have examined the size distribution of SSAs generated in the laboratory and measured in field campaigns (Mårtensson et al., 2003; Clarke et al., 2006; Sellegri et al., 2006; Keene et al., 2007; Tyree et al., 2007; Norris et al., 2008; Fuentes et al., 2010). In a review of SSA emission measurements from both laboratory- and field-based studies, de Leeuw et al. (2011) showed a broad range (0.05–0.1 μm in dry diameter) of particle sizes having the maximum number production flux. Recent SSA production parameterizations (see Grythe et al., 2014) reflect these measurements, with most having a production rate maximum at aerosol sizes lower than the lower cutoff (0.07 μm dry diameter) of Gong (2003). Recent updates to the SSA emission parameterization in the Weather Research and Forecasting model coupled with chemistry (WRF–Chem) increased predicted submicron sodium mass concentrations over the northeastern Atlantic Ocean by up to 20 % (Archer-Nicholls et al., 2014). Due to the lack of detailed submicron measurements at the time, the Gong (2003) parameterization was given as

$$\frac{dF}{dr} = 1.373 U_{10}^{3.41} r^{-(4.7(1+\Theta)r^{-0.017r^{-1.44}})} (1 + 0.057r^{3.45}) \times 10^{1.607e^{-((0.433-\log r)/0.433)^2}}, \quad (1)$$

where $\frac{dF}{dr}$ is the SSA number flux with units of $\text{m}^{-2} \text{s}^{-1} \mu\text{m}^{-1}$, r is the particle radius in μm at 80 % relative humidity, U_{10} is the 10 m wind speed in m s^{-1} , and Θ is an adjustable shape parameter that controlled the submicron size distribution. Gong (2003) tested Θ values between 15 and 40, suggesting (with limited observational evidence) a Θ value of 30.

Seawater temperature can increase or decrease SSA number emissions by up to ~ 100 % due to the temperature dependency of surface tension, density, viscosity, and air entrainment (Mårtensson et al., 2003; Sellegri et al., 2006; Zábóri et al., 2012a; Ovadnevaite et al., 2014; Callaghan et al., 2014). Mårtensson et al. (2003), Sellegri et al. (2006), and Zábóri et al. (2012a) all observed a negative temperature dependence for the production flux of SSAs < 70 nm diameter in synthetic seawater laboratory experiments. Similar negative temperature dependencies are measured in SSAs generated from Arctic Ocean seawater (Zábóri et al., 2012b). Mårtensson et al. (2003) and Sellegri et al. (2006) also reported positive temperature dependencies for the SSA pro-

duction flux for particles larger than 70 nm in diameter. This difference in the temperature dependence of small and large SSA emissions is likely due to their bubble size dependence and impact of SSTs on small and large bubbles (Sellegri et al., 2006). Sofiev et al. (2011) developed a size-dependent temperature correction factor for SSA emissions reflecting the different temperature dependencies of fine- and coarse-mode aerosols. A global comparison of observed and model-predicted coarse-mode sea salt concentrations in Jaeglé et al. (2011) led to the development of a third-order polynomial function for the SST dependence of the Gong (2003) SSA emission parameterization. Grythe et al. (2014) compares the Jaeglé et al. (2011) and Sofiev et al. (2011) temperature dependencies, finding that the Jaeglé et al. (2011) function gives the best model improvement to the observed temperature dependence. Modeling studies implementing the Jaeglé et al. (2011) temperature-dependent SSA emissions have shown improved prediction of surface sea salt mass concentration (Spada et al., 2013; Grythe et al., 2014) relative to temperature-independent emissions. Using a process-based approach incorporating seawater viscosity and wave state, Ovadnevaite et al. (2014) found a positive temperature dependence of SSA emissions similar to Jaeglé et al. (2011) but resembling a linear (rather than third-order polynomial) relationship.

In addition to bubble bursting in the open ocean, SSAs can be emitted via wave breaking in the surf zone covering an area roughly 20 to 100 m from the coastline (Petelski and Chomka, 1996; Lewis and Schwartz, 2004). Surf-zone SSA emissions have been shown to be enhanced relative to the open ocean, resulting in higher sea salt concentrations near the coast (de Leeuw et al., 2000). Vignati et al. (2001) concluded that surf-zone SSA emissions provide additional surface for heterogeneous reactions and impact the atmospheric chemistry of coastal areas. There are limited observations and large uncertainties in the surf-zone SSA emissions related to the zone width and whitecap coverage, with de Leeuw et al. (2000) observing a 30 m wide surf zone with an assumed 100 % whitecap fraction on the California coast and Clarke et al. (2006) observing a mean whitecap fraction in the 35 m wide surf zone of 40 % in Hawaii. The inclusion of surf-zone emissions increases sodium and chloride concentrations by a factor of 10 and improves the predicted concentration of particulate matter (PM) $< 10 \mu\text{m}$ in diameter (PM₁₀) by up to 20 % in the eastern Mediterranean (Im, 2013).

The current SSA treatment in the Community Multiscale Air Quality (CMAQ) model version 5.0.2 is described by Kelly et al. (2010) and includes the open-ocean emissions of Gong (2003), surf-enhanced emissions similar to de Leeuw et al. (2000) in which a fixed whitecap coverage of 100 % is applied to the Gong (2003) parameterization for a 50 m wide surf zone, and dynamic transfer of HNO₃, H₂SO₄, HCl, and NH₃ between coarse-mode particles and the gas phase. Based on comparison with observations from three Tampa,

Florida sites at different distances from the coastline, Kelly et al. (2010) found that enhancing sea spray emissions in surf-zone-containing grid cells by assuming a 50 m wide surf-zone width and 100 % whitecap coverage improved CMAQ model underprediction of sodium, chloride, and nitrate concentrations (particularly at the coastal site) relative to a simulation with only the Gong (2003) open-ocean emissions. The dynamic transfer of HNO_3 , H_2SO_4 , HCl , and NH_3 between coarse particles and the gas phase as implemented by Kelly et al. (2010) further improves predicted concentrations of semi-volatile species like chloride and nitrate. Despite these improvements, persistent underpredictions of sodium, chloride, and nitrate concentrations at the inland site remain unresolved. In this work, we expand upon the Kelly et al. (2010) CMAQ SSA emission treatment by updating the fine-mode size distribution, SST dependence, and surf-enhanced emissions to reflect recent SSA research. Due to the advanced treatment of SSA chemistry in CMAQ, their emissions can be evaluated using concentrations of the directly emitted sea salt components such as sodium and species such as nitrate that react with sea salt components in the atmosphere. Specifically, we hypothesize that the improved prediction of sodium will correspond to improvements in the gas-particle partitioning of nitrate aerosol as suggested by Kelly et al. (2014). The goal of this work is to improve the size distribution, magnitude, and spatiotemporal variability of CMAQ-predicted SSA emissions and the resulting impacts on atmospheric chemistry in coastal and inland areas.

2 Methods

2.1 Observational data sets

Two field campaigns with different meteorology, atmospheric chemistry, and SSA sources from oceans having distinct surface temperatures and bathymetry were used to evaluate the updated emissions. The Bay Regional Atmospheric Chemistry Experiment (BRACE) (Atkeson et al., 2007; Nolte et al., 2008) was conducted from May to June 2002 at three sites (Azalea Park: 27.78° N, 82.74° W; Gandy Bridge: 27.89° N, 82.54° W; and Sydney: 27.97° N, 82.23° W) around Tampa Bay, FL (see Fig. 1). These three sites represent coastal (Azalea Park), bayside (Gandy Bridge), and inland (Sydney) regions, and roughly 1, 25, and 50 km from the Gulf of Mexico coastline. Size-resolved measurements of inorganic PM composition were made with four micro-orifice cascade impactors, which operated for 23 h per sample at ambient relative humidity (Evans et al., 2004). The cascade impactors had 8–10 fractionated stages ranging from 0.056 to 18 μm in aerodynamic diameter, and two cascade impactors were collocated at the Sydney site. Additionally, particulate nitrate and nitric acid were measured under ambient relative humidity conditions at a high temporal resolution (≤ 15 min) using a soluble particle collector employing ion

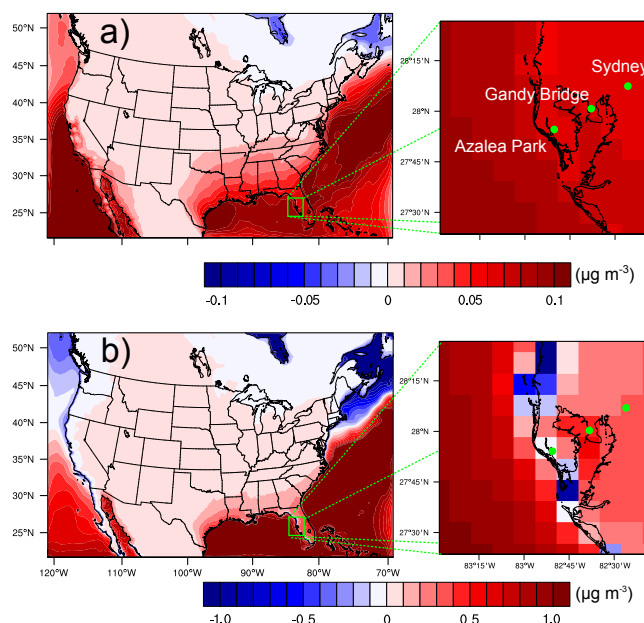


Figure 1. Change in the (a) fine mode and (b) total surface sodium concentration between the revised and baseline simulations for May 2002 over the continental US and BRACE domains with sites from left to right: Azalea Park, Gandy Bridge, and Sydney as green dots.

chromatography (Dasgupta et al., 2007) and denuder difference (Arnold et al., 2007).

The California Research at the Nexus of Air Quality and Climate Change (CalNex) 2010 field project was conducted from May to July 2010 throughout California. The goal of the study was to simultaneously measure variables affected by emissions, atmospheric transport and dispersion, atmospheric chemical processing, and cloud–aerosol interactions and aerosol radiative effects (Ryerson et al., 2013). The South Coast portion of the CalNex campaign included continuous ground-based measurements of $\text{PM} < 2.5 \mu\text{m}$ in diameter ($\text{PM}_{2.5}$) composition using particle-into-liquid sampling and ion chromatography (Weber et al., 2001) and the mixing ratio of many gases at Pasadena, CA (34.14° N, 118.12° W; ~ 35 km from the Pacific coast). Here, we evaluated CMAQ for June 2010 to coincide with surface concentrations of sodium and nitrate measured continuously at Pasadena and as daily averages every 3 days at sites operated by the national Chemical Speciation Network (CSN) within the South Coast, San Francisco Bay, and San Diego air basins. Hereafter, these CSN sites and the Pasadena site will collectively be referred to as the coastal CalNex sites. Although the CalNex campaign also included ship-based measurements of aerosol composition in conjunction with the Sea Sweep (Bates et al., 2012; Crisp et al., 2014), the portion of the cruise that took place in June 2010 was mainly in the vicinity of San Francisco Bay in close proximity to several CSN sites already included in the evaluation. For the CalNex comparison, the sum of the Aitken and accumulation modes

was used as the model comparison. However, a comprehensive evaluation of size-resolved inorganic particle composition from Nolte et al. (2015) shows that the difference in the sum of the Aitken and accumulation modes and $\text{PM}_{2.5}$ values is $< 10\%$.

In addition to local field campaigns, we evaluated SSA emissions in CMAQ against surface $\text{PM}_{2.5}$ concentrations of sodium and nitrate measured throughout the continental US (CONUS) as part of the Interagency Monitoring of Protected Visual Environments (IMPROVE) for remote/rural locations and CSN for urban locations during the May 2002 BRACE time period. Daily average sodium mass concentrations in the IMPROVE and CSN networks were measured once every 3 days via tube-generated X-ray fluorescence (XRF) (White, 2008). Nitrate concentrations for both the IMPROVE and CSN networks are determined by ion chromatography. During the May 2002 period, the IMPROVE network consisted of ~ 160 sites while the CSN network consisted of ~ 230 sites. Although we use the filter-based measurements from the IMPROVE and CSN networks and BRACE campaign for direct model evaluation, we acknowledge that they have uncertainties related to instrument sensitivity and volatility (White, 2008).

2.2 Model configuration

In this work, we used the CMAQ model v5.0.2 to simulate the impact of updated sea spray aerosol emissions on surface aerosol concentrations/size distribution and gas-particle partitioning. CMAQ represents the aerosol size distribution using three modes (Aitken, accumulation, and coarse) and simulates inorganic aerosol thermodynamics using ISORROPIA II (Binkowski and Roselle, 2003; Fountoukis and Nenes, 2007). Kelly et al. (2010) further enhanced the SSA chemical treatment in CMAQ by allowing dynamic transfer of HNO_3 , H_2SO_4 , HCl , and NH_3 between coarse particles and the gas phase. For comparison with the CONUS observational data sets such as IMPROVE and CSN, we used a model domain covering the continental US at $12\text{ km} \times 12\text{ km}$ horizontal resolution and 41 vertical layers with a surface layer up to 20 m a.g.l. The simulation time period (1 May 2002 to 3 June 2002 with an 11 day spin-up) was made to coincide with the BRACE campaign to enable additional evaluation of the coastal-to-inland changes in the aerosol composition/size distribution and gas-particle partitioning. Meteorological parameters were generated by the Weather Research Forecasting model (WRF) version 3.1 (Skamarock et al., 2008), with initial and boundary conditions generated from a previous CMAQ simulation and a GEOS-Chem global model simulation, respectively. Detailed meteorological and emission inputs can be found in Bash et al. (2013). For the CalNex comparison, we used a model domain covering nearly all of California and Nevada as well as parts of the Pacific Ocean, Mexico, and Arizona with 4 km horizontal resolution and 34 vertical layers. Chemical boundary conditions were derived

from a GEOS-Chem simulation (Henderson et al., 2014), and prognostic meteorological fields used to drive CMAQ were generated with WRF version 3.4. Detailed description of the meteorological and emission inputs can be found in Baker et al. (2013) and Kelly et al. (2014). SST was taken from the Moderate Resolution Imaging Spectroradiometer (MODIS) composite for all simulations.

As the Θ value primarily affects the fine-mode size distribution of the Gong (2003) SSA production parameterization, adjusting Θ allows the user to change the (1) number flux without affecting the mass flux and (2) peak aerosol size emitted (see Fig. S1 in the Supplement). These two changes can result in higher downwind concentrations of sea salt components due to the reduced dry deposition velocities of fine-mode aerosols relative to the coarse mode and resulting increase in atmospheric lifetime. The higher downwind concentration of sodium aerosol can increase the concentration of nitrate aerosol by affecting the gas-particle partitioning of total inorganic nitrate ($\text{NO}_3^- + \text{HNO}_3$). This increase, in turn, can increase the nitrate lifetime as fine-mode NO_3^- has a longer atmospheric lifetime than gaseous HNO_3 . Both the sea salt and nitrate aerosol concentrations at the Sydney inland site were found to be underpredicted in CMAQ (Kelly et al., 2010). For this study, we used Θ values of 30 (consistent with the current CMAQ representation, given as CMAQv5.0.2a or “baseline”), 20 (CMAQv5.0.2b), 10 (CMAQv5.0.2c), and 8 (CMAQv5.0.2d), which were expected to result in progressively higher emission rates of fine-mode SSAs (see Fig. S1). For the simulations using Θ values ≤ 20 , the lower limit of the SSA dry diameter is decreased to 10 nm to better reflect changes in the emitted number size distribution (which peaks at ~ 170 , 140, 80, and 60 nm dry diameter for Θ values of 30, 20, 10, and 8, respectively). This decrease was consistent with measurements of Aitken mode SSAs (Clarke et al., 2006) and a recent global modeling study evaluating different SSA emission parameterizations (Grythe et al., 2014). The radius of peak emissions at 80% relative humidity (RH) from the Gong (2003) parameterization with a Θ value of 8 was ~ 60 nm; this value was similar to the radius of maximum production flux from several parameterizations reviewed in de Leeuw et al. (2011).

Including the positive temperature dependence for SSA emissions in CMAQ was expected to affect the seasonality and spatial distribution of predicted concentrations. The Jaeglé et al. (2011) third-order polynomial function of SST dependence for SSA emissions (CMAQv5.0.2e) increases the summertime/tropical concentrations, decreases wintertime/polar concentrations, and leaves mid-latitude/spring/autumn concentrations relatively unchanged. The surf-zone width used in parameterizing the surf-enhanced emissions was decreased from 50 to 25 m (CMAQv5.0.2f), reflecting both the uncertainty in the width distance and whitecap fraction within the surf zone. As SSA emissions from surf-zone-containing grids impact a narrow region, adjusting the surf-zone width was expected to

Table 1. Differences in the CMAQ model versions used in this study.

Simulation	Θ	SST dependence	Surf Zone (m)
Baseline ¹	30	None	50
CMAQv5.0.2b	20	None	50
CMAQv5.0.2c	10	None	50
CMAQv5.0.2d	8	None	50
CMAQv5.0.2e	30	Jaeglé et al. (2011)	50
CMAQv5.0.2f	30	None	25
CMAQv5.0.2g	8	Jaeglé et al. (2011)	25
Revised ²	8	Jaeglé et al. (2011), Ovadnevaite et al. (2014)	25

¹ This simulation is also referred to as the CMAQv5.0.2a simulation. ² In this simulation, which is also referred to as the CMAQv5.0.2h simulation, the SST dependence of Jaeglé et al. (2011) has been linearized following Ovadnevaite et al. (2014).

strongly affect coastal concentrations while having a relatively minor effect on downwind concentrations. We conducted two simulations to test the combined effect of setting $\Theta = 8$, SST dependence, and surf-enhanced emissions (surf zone = 25 m), with CMAQv5.0.2g using the Jaeglé et al. (2011) third-order SST dependence and CMAQv5.0.2h using a hybrid of the Jaeglé et al. (2011) third-order SST dependence and the Ovadnevaite et al. (2014) process-based linear SST dependence (see Fig. 12 from Ovadnevaite et al., 2014) for open-ocean emissions as follows:

$$\frac{dF}{dr} = (0.38 + 0.054 \times \text{SST}) \times 1.373 U_{10}^{3.41} r^{-(4.7(1+8r)^{-0.017r-1.44})} (1 + 0.057r^{3.45}) \times 10^{1.607e^{-((0.433-\log r)/0.433)^2}}, \quad (2)$$

where SST has units of °C. The updated SSA emission parameterization given in Eq. (2) was mapped to the CMAQ aerosol modes as a function of relative humidity following Zhang et al. (2005, 2006). A summary of the different CMAQ model simulations in which SSA emissions were changed is given in Table 1. The approach used in CMAQv5.0.2h, hereafter referred to as the “revised” simulation, is planned to be included in the next public release of CMAQ (version 5.1).

A potential limitation of this study is the reliance on ambient surface concentrations in the evaluation of modeled SSA emissions. Although all model processes other than SSA emissions are left constant for the CMAQ simulations listed above, the selection of deposition, transport, and chemistry parameterizations within the model can affect the predicted concentrations. Nolte et al. (2015) found that constraining the aerosol mode widths and enabling gravitational settling for all model layers in CMAQ affected the predicted coarse-mode sodium at the BRACE sites. Although changes in the model chemistry would likely have a minor impact on the

Na⁺ evaluations, future diagnostic evaluations that account for deposition and transport uncertainties are advised.

3 Results

3.1 BRACE

The total particulate (PM_{tot}) nitrate, chloride, and sodium concentrations observed at the three sites during the BRACE campaign and corresponding CMAQ-predicted concentrations for the baseline and sensitivity simulations (v5.0.2b–h) are summarized in Table 2. The baseline simulation predicted the magnitude of chloride and sodium at the coastal site (Azalea Park) relatively well with normalized mean biases (NMBs) between 0 and 25 %. However, it increasingly underpredicted chloride and sodium as the distance from the shore increased (at the inland Sydney site the sodium NMB was −41 %). The baseline simulation overestimated by approximately a factor of 2 the observed decrease in PM_{tot} chloride and sodium between the coastal Azalea Park and inland Sydney sites. The average fine-mode sodium concentration (given as PM_{1.8} for the measurements and the sum of the Aitken and accumulation approximating PM_{2.5} (Nolte et al., 2015) for the model predictions) was consistently underpredicted by the baseline simulation for the BRACE sites with an NMB of −21.6 %. The baseline simulation underpredicted nitrate concentrations for all sites with a NMB of −46.4 %. As the Θ value was changed from 30 to 20 (v5.0.2b), the predicted PM_{tot} chloride and sodium (and nitrate via secondary processes) at the coastal Azalea Park site decreased slightly (< 0.1 μg m^{−3}) despite an increase (by 0.05 μg m^{−3}) in fine-mode sodium concentrations. This surprising result was due to slight differences in the fitting of coarse-mode SSA emissions to CMAQ’s aerosol modes. The transition of Θ values from 20 to 10 to 8 led to small (~0.05 to 0.1 μg m^{−3}, or 10 %) increases in the nitrate, chloride, and sodium concentrations relative to the baseline simulation for all sites. Although it slightly overestimated chloride and sodium at the coastal Azalea Park site, the v5.0.2d simulation with a Θ value of 8 had the best prediction (both in terms of magnitude and correlation according to Table 2) of concentrations at the Gandy Bridge and Sydney sites.

The modeled chloride and sodium aerosol concentrations were much more sensitive to the implementation of SST-dependent SSA emissions (v5.0.2e) and reduction of the surf-zone width used for surf-enhanced SSA emissions (v5.0.2f) than the changing of the Θ values. With the positive temperature dependence of the Jaeglé et al. (2011) sea spray aerosol emissions and warm (25 °C) Gulf of Mexico surface waters in May (see Fig. S2), concentrations of nitrate, chloride, and sodium were predicted to be higher (> 20 %) in the v5.0.2e simulation than the baseline for all sites. The reduction in surf-enhanced emissions in the v5.0.2f simulation had a more site-specific impact on surface concentrations,

Table 2. Comparison of the mean and Pearson's correlation coefficient (r) of total observed and model-predicted inorganic particle concentrations ($\mu\text{g m}^{-3}$) at three Bay Regional Atmospheric Chemistry Experiment (BRACE) sites near Tampa, FL.

Species	Obs.	Baseline ^a		v5.0.2b		v5.0.2c		v5.0.2d		v5.0.2e		v5.0.2f		v5.0.2g		Revised ^b	
		Mean	r	Mean	r	Mean	r	Mean	r	Mean	r	Mean	r	Mean	r	Mean	r
Azalea Park																	
NO ₃ ⁻	1.96	0.74	0.34	0.72	0.33	0.73	0.34	0.76	0.35	0.92	0.30	0.65	0.45	0.74	0.45	0.79	0.43
Cl ⁻	1.93	2.41	0.17	2.33	0.15	2.36	0.15	2.49	0.18	3.69	0.19	1.55	0.31	1.92	0.38	2.15	0.42
Na ⁺	1.62	1.62	0.19	1.61	0.18	1.62	0.18	1.71	0.21	2.39	0.22	1.11	0.33	1.38	0.41	1.52	0.44
Na ⁺ c	0.13	0.11	0.38	0.16	0.42	0.15	0.41	0.16	0.42	0.15	0.42	0.10	0.43	0.16	0.53	0.18	0.58
Gandy Bridge																	
NO ₃ ⁻	1.74	1.32	0.55	1.03	0.54	1.03	0.54	1.07	0.55	1.32	0.51	0.93	0.60	1.09	0.61	1.17	0.61
Cl ⁻	1.72	1.57	0.71	1.51	0.71	1.53	0.71	1.63	0.71	2.53	0.68	1.32	0.81	1.91	0.81	2.26	0.81
Na ⁺	1.46	1.17	0.67	1.17	0.67	1.17	0.67	1.24	0.67	1.78	0.65	1.01	0.79	1.41	0.81	1.62	0.80
Na ⁺ c	0.13	0.09	0.51	0.13	0.54	0.12	0.53	0.13	0.54	0.12	0.51	0.09	0.56	0.14	0.60	0.17	0.63
Sydney																	
NO ₃ ⁻	1.51	0.73	0.58	0.71	0.57	0.72	0.57	0.75	0.58	0.88	0.59	0.68	0.60	0.78	0.63	0.84	0.64
Cl ⁻	1.31	0.82	0.35	0.78	0.35	0.79	0.35	0.86	0.36	1.32	0.30	0.71	0.49	1.02	0.50	1.26	0.53
Na ⁺	1.14	0.67	0.44	0.66	0.45	0.67	0.45	0.72	0.46	0.98	0.41	0.59	0.55	0.82	0.57	0.98	0.61
Na ⁺ c	0.11	0.09	0.19	0.12	0.27	0.11	0.25	0.12	0.27	0.11	0.21	0.08	0.23	0.13	0.33	0.16	0.40

^a This simulation is also referred to as the CMAQv5.0.2a simulation. ^b This simulation is also referred to as the CMAQv5.0.2h simulation. ^c Na⁺ predicted for the sum of Aitken and accumulation modes (approximating PM_{2.5}; Nolte et al., 2015) and observed for aerosols < 1.8 μm in diameter.

with the coastal Azalea Park site having a 0.4–0.5 $\mu\text{g m}^{-3}$ (30 %) decrease in predicted chloride and sodium concentrations and the bayside (Gandy Bridge) and inland (Sydney) sites having only a 10–15 % decrease relative to the baseline simulation. Figure S3 shows the model grid cells in the vicinity of Tampa Bay (including the Gandy Bridge site) have a representation of the open-ocean fraction but not the surf-zone fraction used for surf-enhanced SSA emissions. The predicted 50 % decrease in the chloride and sodium surface concentrations from Azalea Park to Sydney in the v5.0.2f simulation was more similar to the observed 30 % decrease than the 60 % decrease predicted by the baseline simulation.

In general, the best model performance at the BRACE sites occurred with SSA emissions having a Θ value of 8, SST dependence, and a reduced surf enhancement as implemented in the v5.0.2g and revised simulations. While both the v5.0.2g and revised simulations severely underpredicted nitrate concentrations (by up to 1.2 $\mu\text{g m}^{-3}$) at all sites, the chloride and sodium concentrations were consistently improved both in magnitude and correlation compared to the baseline simulation (see Table 2). The largest improvement occurred at the inland Sydney site, where substantial underpredictions of chloride and sodium in the baseline simulation were largely eliminated in the revised simulations (chloride and sodium NMBs improved from $-37/ -41$ % to $-4/ -14$ %, respectively). Comparison of the simulations with the third-order polynomial (v5.0.2g) and linear (revised) SST dependence of SSA emissions revealed that the linear dependence led to slightly improved prediction of chloride and sodium at the Azalea Park and Sydney sites (Pearson's correlation coefficients jumped from 0.57 to 0.61 and biases

went from -0.32 to -0.16 $\mu\text{g m}^{-3}$ for sodium in Sydney) and similar performance at the Gandy Bridge site. Improved prediction of chloride and sodium concentrations at these sites was not surprising as the linear temperature dependence was adapted from a process-based parameterization incorporating seawater viscosity and wave state (Ovadnevaite et al., 2014) as opposed to the top-down, model-specific third-order polynomial parameterization developed for GEOS-Chem in Jaeglé et al. (2011).

The statistical improvement in the revised simulation relative to the baseline simulation is reflected in the time series of sodium concentrations at the three sites (Fig. 2). Besides showing the generally higher PM_{tot} sodium concentrations at the bayside and inland sites and higher PM_{1.8} sodium concentrations at all sites, Fig. 2 also shows that the revised simulation diverges most from the baseline during periods of high SSA concentration episodes (15, 22 May 2002). This suggests that the revised simulation better replicated the sea spray aerosol emissions during periods with strong on-shore flow compared to the baseline simulation. The range of PM_{1.8} sodium concentrations predicted by the revised simulation was more consistent with observations than the baseline simulation, especially at the Sydney site which has observed concentrations of 0.05–0.27 $\mu\text{g m}^{-3}$ and predicted concentrations of 0.02–0.16 $\mu\text{g m}^{-3}$ and 0.03–0.25 $\mu\text{g m}^{-3}$ for the baseline and revised simulations. The PM_{1.8} sodium concentrations at the BRACE sites were lower than PM_{2.5} sodium measured at a nearby CSN site (located at 28.05° N, 82.378056° W) averaging 0.34 $\mu\text{g m}^{-3}$ during the same period but well correlated (correlation coefficients ranging from 0.65 to 0.90) for the 5–6 days of coincident measurements.

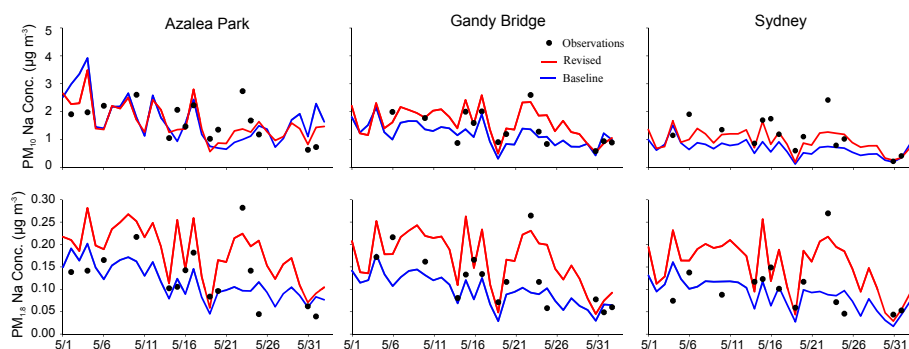


Figure 2. Time series of the observed and predicted daily PM_{10} and $\text{PM}_{1.8}$ Na^+ concentration at the three BRACE sites. Note that the $\text{PM}_{1.8}$ Na^+ concentration predicted by CMAQ is represented by the sum of the Aitken and accumulation modes.

This CSN site is part of the CONUS model evaluation described in Sect. 3.3.

Comparison of the predicted and observed size distribution of sodium at the three sites (see Fig. 3) showed that much of the observed and predicted decrease in the sodium mass concentration in the transition from coastal to inland sites occurred within the coarse mode. The baseline simulation overpredicted/underpredicted coarse-mode sodium at the coastal/inland sites, while the revised simulation well predicted the coarse-mode sodium at both the coastal and inland sites. At the bayside Gandy Bridge site, the high SSTs in Tampa Bay resulted in an increase in the bias from the baseline simulation due to the revised simulation overestimating coarse-mode observations. Both the baseline and revised simulations predict a second submicron mode for the three sites that is not evident in the observations; it is unclear whether this discrepancy is related to inaccuracies in the size-resolved emissions or the modal distribution of the model.

Fine-mode (Aitken + accumulation) sodium concentrations increased throughout the BRACE domain in the revised simulation relative to the baseline simulation with larger changes (up to $0.1 \mu\text{g m}^{-3}$) offshore and smaller changes ($0.05 \mu\text{g m}^{-3}$) inland as shown in the right column of Fig. 1a. The total (sum of Aitken, accumulation, and coarse modes) sodium concentrations over the open ocean increased in the warmer southern waters of the Atlantic and Pacific oceans and decreased in the cooler waters off New England and the Pacific Northwest. Grid cells directly adjacent to the coast experienced concentration decreases of up to $1 \mu\text{g m}^{-3}$, with the largest decreases occurring for cells with large surf zones due to irregular coastlines (barrier islands, peninsulas, etc.). These coastline-centered decreases were limited spatially, as adjacent cells just offshore had large increases in sodium concentration. Like the fine-mode changes, the largest total sodium concentration increases occurred offshore while more modest increases were predicted for inland locations. The coastal-inland concentration gradients were stronger for the total concentration changes due to the faster deposition

velocity of coarse-mode aerosols (relative to the fine mode) that comprise most of the total mass.

The hourly time series of observed and predicted nitrate gas/particle partitioning from the Sydney site for May 2002 (Fig. 4) shows that the revised simulation pushes the partitioning towards the particle phase (relative to the baseline simulation) and closer to observations. The average observed fraction of nitrate in the particle phase was 0.51, while the predicted fractions from the baseline and revised simulations were 0.36 and 0.42, respectively. Figure 4 indicates that the largest difference in the nitrate partitioning between the baseline and revised simulations occurred during the daytime, when higher concentrations of inorganic ions like sodium prevented some of the nitric acid evaporation from the particle phase during the hot afternoon period. Despite improvement in the daytime partitioning, the revised simulation continued to overpredict the nighttime nitrate fraction and daytime nitric acid fraction. This impact on partitioning is consistent with Kelly et al. (2014), which suggested that improving CMAQ prediction of sodium concentration and relative humidity would improve gas-particle partitioning of nitrate in the CalNex model domain.

3.2 CalNex

Similar to results for the BRACE sites, the predicted fine-mode sodium surface concentrations were improved in the revised simulation relative to the baseline for sites examined during the CalNex simulation period (see Fig. 5). Surface sodium concentrations were underpredicted by both the baseline and revised simulations for all the coastal CalNex sites, especially in the 11–16 June time period when high sodium concentrations at several of the sites were not well captured by either the revised or baseline simulation. It is worth noting that a sensitivity test in which the surf-enhanced emissions were increased (using a surf-zone width of 100 m rather than 25 m as in the revised simulation) did not substantially improve the sodium underpredictions at the coastal CalNex sites. Monthly average (June 2010) sodium concentrations predicted in the revised simulation increased

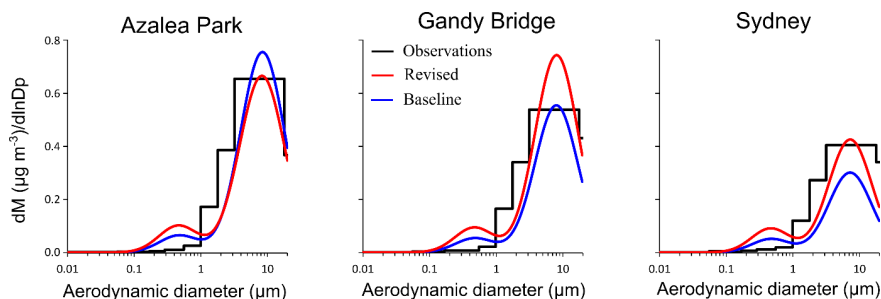


Figure 3. Observed and predicted size distributions of Na^+ at the three Tampa-area sites averaged over 15 sampling days (14 at Sydney) during 2 May–2 June 2002.

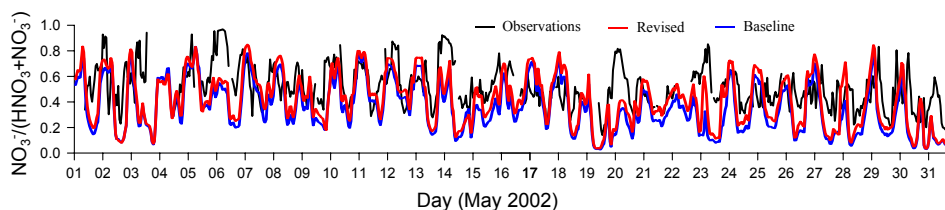


Figure 4. Time series of observed and modeled fraction of total nitrate in the particle phase $[\text{NO}_3^- / (\text{HNO}_3 + \text{NO}_3^-)]$ at the Sydney, FL, site for May 2002. Tick marks represent 00:00 local standard time on each day.

by up to $\sim 0.25 \mu\text{g m}^{-3}$ off the California coast relative to the baseline simulation, with increases between 0.05 and $0.1 \mu\text{g m}^{-3}$ widespread in the San Francisco, Los Angeles, and San Diego air basins (Fig. 5). Hourly or daily average increases between the revised and baseline simulations were even higher in these urban areas, with the time series plots in Fig. 5 showing increases up to $0.2 \mu\text{g m}^{-3}$. The spatial patterns of impacts on sodium in the Central Valley and South Coast air basin matched those of tracers released from San Francisco and LAX airport that are drawn inland on the sea breeze (Baker et al., 2013).

Improving the sodium underprediction at the coastal CalNex sites in the revised simulation had the effect of improving the frequent nitrate aerosol underprediction at the same sites (see Fig. 6). Unlike the sodium concentration changes, the largest ($0.5 \mu\text{g m}^{-3}$) increases in monthly average nitrate aerosol concentration occurred over the Los Angeles air basin well inland from the coast. The increase of nitrate largely occurred in inland areas where nitric acid was produced downwind of urban centers with large NO_x emissions. For conditions unfavorable for ammonium nitrate formation (e.g., high temperature, low RH, low NH_3), nitrate may still form in sea spray particles through replacement reactions (e.g., $\text{NaCl(p)} + \text{HNO}_3(\text{g}) \rightarrow \text{NaNO}_3(\text{p}) + \text{HCl}(\text{g})$). Since such pathways involve pollution derived from urban emissions (HNO_3) in addition to sea salt (NaCl), the highest nitrate increases occurred inland despite the relatively small increases in sodium compared to the baseline simulation in these areas. Similarly, polluted sites such as Pasadena and Riverside had larger increases in nitrate concentrations than

cleaner sites in the San Francisco air basin despite having similar sodium concentration changes. This behavior suggested that these SSA emission updates had the largest air quality impact in coastal urban areas with mixtures of marine and polluted air masses. Note that the nitrate-to-sodium ratio of molar masses is about 2.7, and so a 1 : 1 increase in the moles of sodium and nitrate according to NaNO_3 stoichiometry would lead to a greater increase of nitrate than sodium mass. The nitrate underpredictions in Fig. 6 were not resolved entirely by improved sodium predictions. In Riverside, for example, nitrate underpredictions in the revised simulation were likely due to a combination of persistent sodium underpredictions and an underestimate of ammonia emissions from upwind dairy facilities (Nowak et al., 2012; Kelly et al., 2014).

3.3 Continental US

Unlike the $\text{PM}_{1.8}$ or $\text{PM}_{2.5}$ -sodium concentrations evaluated using the BRACE and CalNex observations, the total sodium surface concentration changes shown in Fig. 1b both increased and decreased in the CONUS domain due to the variability in coastal and oceanic SSTs. The distribution of fine-mode (Aitken + accumulation) concentration changes (Fig. 1a) had some similar features to the total concentration changes (Fig. 1b), with the largest increases occurring over areas with high ($> \sim 20^\circ\text{C}$) SSTs. Differences between the fine mode and total concentration changes were most notable for regions with low ($< \sim 10^\circ\text{C}$) SSTs (Pacific and northeastern US coasts) and for inland regions. Because fine-mode particles have a low dry deposition velocity, off-

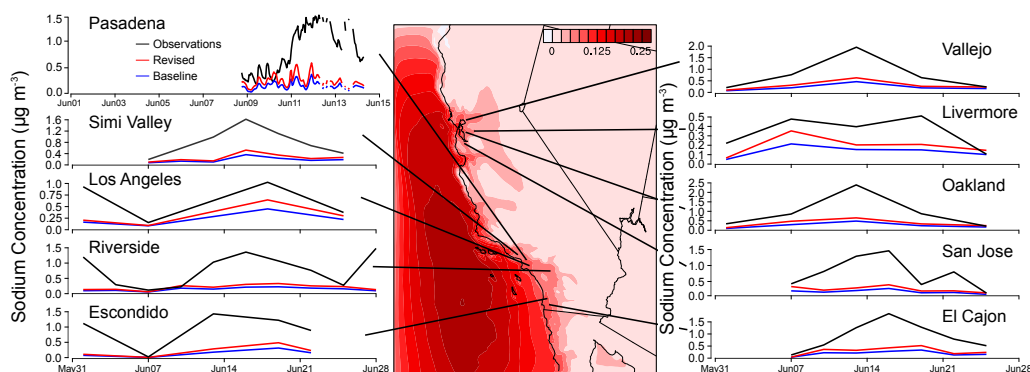


Figure 5. Change ($\mu\text{g m}^{-3}$) in the fine-mode (Aitken + accumulation) surface sodium concentration between the revised and baseline simulations for June 2010 over the CalNex domain surrounded by time series plots of the observed and predicted daily and/or hourly $\text{PM}_{2.5}$ -sodium concentration at the coastal CalNex sites.

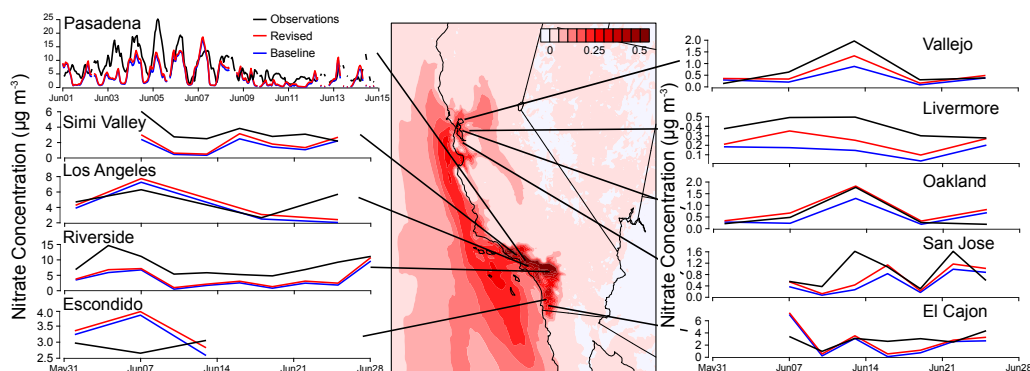


Figure 6. Change ($\mu\text{g m}^{-3}$) in the fine-mode (Aitken + accumulation) surface nitrate concentration between the revised and baseline simulations for June 2010 over the CalNex domain surrounded by time series plots of the observed and predicted daily and/or hourly $\text{PM}_{2.5}$ nitrate concentration at the coastal CalNex sites.

shore increases in the fine-mode sodium concentrations were able to extend inland and lead to increased deposition (see Fig. S4a). The flat topography and large offshore concentration increases in the southeastern US resulted in concentration increases of up to $0.25 \mu\text{g m}^{-3}$ hundreds of kilometers from the coast. While reductions in fine-mode SSA emissions due to low SSTs were balanced by increased emissions from changing Θ , cold seawater temperatures off the Pacific coast and northeastern US led to large decreases in total sodium concentration of up to $-0.5 \mu\text{g m}^{-3}$. As in the BRACE domain, the decrease in surf-enhanced emissions led to localized decreases in PM_{tot} sodium concentration for grid cells immediately adjacent to the coastline throughout the CONUS domain. Regions with rugged coastlines and barrier islands experienced the largest concentration decreases because of the large surf-zone area.

Model comparison of $\text{PM}_{2.5}$ -sodium concentrations from the IMPROVE and CSN networks revealed improvement from the baseline to revised simulation (see Fig. 7). For both the IMPROVE and CSN networks, far fewer sites had an increased error (Fig. 7a) in the revised simulation relative to the baseline than had reductions in the model error (Fig. 7b).

Table 3. Statistical comparison of the mean and Pearson’s correlation coefficient (r) between observed and model-predicted sodium, nitrate and $\text{PM}_{2.5}$ surface concentrations ($\mu\text{g m}^{-3}$) for the continental US in May 2002 from the IMPROVE and CSN networks.

Specie	Obs.	Baseline ¹		v5.0.2g		Revised ²	
		Mean	r	Mean	r	Mean	r
IMPROVE							
Na^+	0.44	0.16	0.11	0.16	0.17	0.19	0.20
NO_3^-	0.61	0.23	0.28	0.26	0.26	0.26	0.27
$\text{PM}_{2.5}$	5.98	4.24	-0.04	4.16	-0.01	4.30	0.04
CSN							
Na^+	0.34	0.11	0.59	0.14	0.62	0.15	0.62
NO_3^-	1.94	0.61	0.76	0.68	0.76	0.68	0.75
$\text{PM}_{2.5}$	9.74	6.04	0.74	6.29	0.74	6.48	0.74

¹ This simulation is also referred to as the CMAQv5.0.2a simulation. ² This simulation is also referred to as the CMAQv5.0.2h simulation.

Sites where the model error increased in the revised simulation were widely scattered across the CONUS domain and typically overpredicted concentrations. The sites where

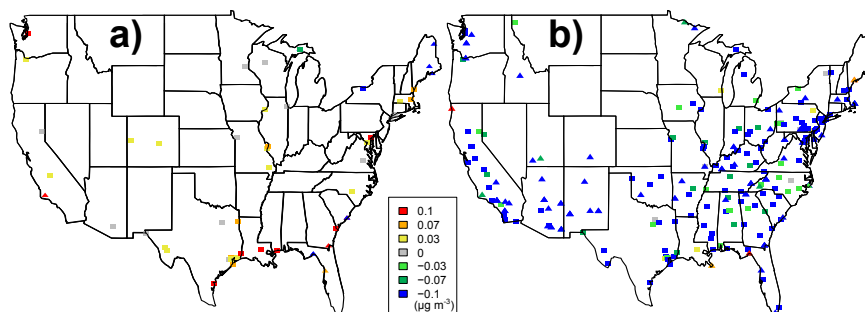


Figure 7. Model bias of $\text{PM}_{2.5}$ -sodium concentration predicted by the revised simulation compared to observations from the IMPROVE (triangles) and CSN (squares) networks for May 2002 segregated by an (a) increase or (b) decrease in the error relative to the baseline simulation. The map only includes data where the model percentage difference between the revised and baseline simulations is $> 5\%$.

model error was reduced in the revised simulation were in the southeastern and mid-Atlantic US and typically underestimated concentrations. Sodium concentrations at numerous sites were underpredicted by $> 0.1 \mu\text{g m}^{-3}$ in the revised simulation, suggesting that the SSA emission changes were insufficient to bring the model into agreement with most observations. Despite cold waters off the Pacific coast leading to lower emissions (relative to the warmer Gulf of Mexico) in the revised simulation, there were more sites in California that had an error reduction in the predicted concentrations than had increased model error. Cold waters in the Gulf of Maine and the associated lower emissions/concentrations in the revised simulation had the effect of reducing the overprediction of sodium at several sites in coastal New England. Table 3 shows that the average bias for sodium concentrations for all stations in the IMPROVE and CSN networks was reduced from the baseline to revised simulation (NMB: -63.7 to -57.6% and -67.2 to -54.9% for the IMPROVE and CSN networks, respectively) with small improvements in the correlation. Predicted nitrate concentrations improved in the revised simulation relative to the baseline, with slight reductions in the large model underpredictions for the IMPROVE (NMB: -62.7 to -56.8%) and CSN (NMB: -68.6 to -65.0%) networks. Despite similar changes in average sodium concentrations between the baseline and revised simulations for the IMPROVE and CSN networks, the average change in $\text{PM}_{2.5}$ between the two simulations was much higher for the CSN ($+0.42 \mu\text{g m}^{-3}$) than the IMPROVE ($+0.06 \mu\text{g m}^{-3}$) network. Predominantly comprised of urban sites, CSN sites are located in more polluted regions where changes in sodium concentrations were more likely to have an impact on the partitioning of HNO_3 , HCl , and NH_3 between gas and particle phases leading to increases in nitrate aerosol concentrations (see Fig. 6 for an example). The enhanced partitioning of nitrate to the particle phase in the revised simulation also led to decreased deposition of total nitrate inland because of the lower dry deposition velocity of nitrate aerosol relative to nitric acid (see Fig. S4b).

4 Conclusions

In this study, the size distribution, temperature dependence, and surf-zone enhancement of sea spray aerosol (SSA) emissions were updated in the Community Multiscale Air Quality (CMAQ) model version 5.0.2. Increasing fine-mode emissions, including temperature dependence, and reducing the surf-enhanced emissions from the “baseline” to the “revised” simulation collectively improved the summertime surface concentration predictions for sodium, chloride, and nitrate at three Bay Regional Atmospheric Chemistry Experiment (BRACE) sites near Tampa, Florida. Surface concentrations at the inland site near Tampa were particularly affected by these emission changes, as low dry deposition velocities for the fine-mode aerosols increased the atmospheric lifetime and inland concentrations. The coastal–inland concentration gradient was also affected by the updated emissions, as the reduction in surf-zone width used to enhance surf-zone emissions brought the revised simulation in closer agreement with observations. These SSA emission updates led to increases in the fine-mode sodium surface concentrations throughout coastal areas of the continental US, with the largest increases occurring near the southeastern US coast where sea surface temperatures (SSTs) were high. Decreases in the total sodium concentration were predicted for oceanic regions with low SSTs such as the Pacific and northern Atlantic coasts. Comparison of the baseline and revised simulation with sodium observations from the IMPROVE and CSN networks showed that the updated emissions reduced the widespread underprediction of concentrations, especially in the southeastern and mid-Atlantic US. Non-linear responses between changes in total and sea salt $\text{PM}_{2.5}$ concentrations indicated that the impacts of these emissions changes on aerosol chemistry were enhanced in polluted coastal environments. The revised simulation had increased sodium and nitrate aerosol concentrations at most CalNex sites, slightly reducing the underprediction from the baseline simulation.

Potential future work includes treating the organic fraction of SSAs (Gantt et al., 2010), implementing the Group for

High Resolution Sea Surface Temperature (GHRSSST) data set (Donlon et al., 2007), and linking the SSA emissions to marine boundary layer halogen chemistry via debromination (Yang et al., 2005). Episodic high SSA concentrations are not well captured at any of the coastal CalNex sites in the revised simulation, suggesting that other factors not accounted for in our updated SSA emission parameterization such as wind history, wave state, ocean biology, solar radiation, whitecap timescales, or the limited ocean surface area in the modeling domain (Callaghan et al., 2008, 2014; Ovadnevaite et al., 2014; Long et al., 2014) may play an important role. Additional model developments focused on the South Coast region of California are warranted considering the impact on nitrate discussed above as well as the impact that reactive chlorine atoms derived from sea spray particles can have on ozone in this region (Simon et al., 2009; Sarwar et al., 2012; Riedel et al., 2014). As the fine-mode size distribution has a far greater impact on the number concentration than the mass concentration, the changes described in this study likely impact other model parameters such as aerosol radiative feedbacks, which are included in the coupled WRF–CMAQ modeling system (Gan et al., 2014).

Code availability

The updated code is available upon request prior to the public release of CMAQ v5.1. Please contact Jesse Bash at bash.jesse@epa.gov for more information.

The Supplement related to this article is available online at [doi:10.5194/gmd-8-3733-2015-supplement](https://doi.org/10.5194/gmd-8-3733-2015-supplement).

Acknowledgements. We would like to acknowledge use of Rodney Weber's continuous PM_{2.5} composition measurements from the Pasadena ground site and monitor data from the IMPROVE and CSN networks. We also thank Christopher Nolte for help in the analysis of the BRACE data set/aerosol size distributions, Kirk Baker for help in the development of the CalNex platform, and the two anonymous reviewers for their constructive comments. The United States Environmental Protection Agency (EPA) through its Office of Research and Development funded and managed the research described here. This paper has been subjected to the Agency's administrative review and approved for publication. B. Gantt is supported by an appointment to the Research Participation Program at the Office of Research and Development, US EPA, administered by ORISE.

Edited by: A. B. Guenther

References

- Andreas, L. E.: A new sea spray generation function for wind speeds up to 32 ms^{-1} , *J. Phys. Oceanogr.*, 28, 2175–2184, 1998.
- Archer-Nicholls, S., Lowe, D., Utembe, S., Allan, J., Zaveri, R. A., Fast, J. D., Hodnebrog, Ø., Denier van der Gon, H., and McFiggans, G.: Gaseous chemistry and aerosol mechanism developments for version 3.5.1 of the online regional model, WRF-Chem, *Geosci. Model Dev.*, 7, 2557–2579, doi:10.5194/gmd-7-2557-2014, 2014.
- Arnold, J. R., Hartsell, B. E., Luke, W. T., Ullah, S. M. R., Dasgupta, P. K., Huey, L. G., and Tate, P.: Field test of four methods for gas-phase ambient nitric acid, *Atmos. Environ.*, 41, 4210–4226, 2007.
- Atkeson, T., Greening, H., and Poor, N.: Bay Region Atmospheric Chemistry Experiment (BRACE), *Atmos. Environ.*, 41, 4163–4164, 2007.
- Baker, K. R., Misenis, C., Obland, M. D., Ferrare, R. A., Scarino, A. J., and Kelly, J. T.: Evaluation of surface and upper air fine scale WRF meteorological modeling of the May and June 2010 CalNex period in California, *Atmos. Environ.*, 80, 299–309, doi:10.1016/j.atmosenv.2013.08.006, 2013.
- Bash, J. O., Cooter, E. J., Dennis, R. L., Walker, J. T., and Pleim, J. E.: Evaluation of a regional air-quality model with bidirectional NH₃ exchange coupled to an agroecosystem model, *Biogeosciences*, 10, 1635–1645, doi:10.5194/bg-10-1635-2013, 2013.
- Bates, T. S., Quinn, P. K., Frossard, A. A., Russell, L. M., Hakala J., Petäjä, T., Kulmala, M., Covert, D. S., Cappa, C. D., Li, S.-M., Hayden, K. L., Nuaaman, I., McLaren, R., Massoli, P., Canagaratna, M. R., Onasch, T. B., Sueper, D., Worsnop, D. R., and Keene, W. C.: Measurements of ocean derived aerosol off the coast of California, *J. Geophys. Res.*, 117, D00V15, doi:10.1029/2012JD017588, 2012.
- Binkowski, F. S. and Roselle, S. J.: Models-3 community multi-scale air quality (CMAQ) model aerosol component – 1. Model description, *J. Geophys. Res.*, 108, 4183–4201, 2003.
- Blot, R., Clarke, A. D., Freitag, S., Kapustin, V., Howell, S. G., Jensen, J. B., Shank, L. M., McNaughton, C. S., and Brekhovskikh, V.: Ultrafine sea spray aerosol over the southeastern Pacific: open-ocean contributions to marine boundary layer CCN, *Atmos. Chem. Phys.*, 13, 7263–7278, doi:10.5194/acp-13-7263-2013, 2013.
- Callaghan, A. H., de Leeuw, G., Cohen, L., and O'Dowd, C. D.: Relationship of oceanic whitecap coverage to wind speed and wind history, *Geophys. Res. Lett.*, 35, L23609, doi:10.1029/2008gl036165, 2008.
- Callaghan, A. H., Stokes, M. D., and Deane, G. B.: The effect of water temperature on air entrainment, bubble plumes, and surface foam in a laboratory breaking-wave analog, *J. Geophys. Res. Oceans*, 119, 7463–7482, doi:10.1002/2014JC010351, 2014.
- Clarke, A. D., Owens, S. R., and Zhou, J. C.: An ultrafine sea-salt flux from breaking waves: Implications for cloud condensation nuclei in the remote marine atmosphere, *J. Geophys. Res.*, 111, D06202, doi:10.1029/2005JD006565, 2006.
- Crisp, T. A., Lerner, B. M., Williams, E. J., Quinn, P. K., Bates, T. S., and Bertram, T. H.: Observations of gas phase hydrochloric acid in the polluted marine boundary layer, *J. Geophys. Res. Atmos.*, 119, 6897–6915, doi:10.1002/2013JD020992, 2014.
- Dasgupta, P. K., Campbell, S. W., Al-Horr, R. S., Ullah, S. M. R., Li, J. Z., Amalfitano, C., and Poor, N. D.: Conversion of sea salt

- aerosol to NaNO_3 and the production of HCl: analysis of temporal behavior of aerosol chloride/nitrate and gaseous HCl/ HNO_3 , *Atmos. Environ.*, 41, 4242–4257, 2007.
- de Leeuw, G., Neele, F. P., Hill, M., Smith, M. H., and Vignati, E.: Production of sea spray aerosol in the surf zone, *J. Geophys. Res.-Atmos.*, 105, 29397–29409, 2000.
- de Leeuw, G., Andreas, E. L., Anguelova, M. D., Fairall, C. W., Lewis, E. R., O'Dowd, C., Schulz, M., and Schwartz, S. E.: Production flux of sea spray aerosol, *Rev. Geophys.*, 49, RG2001, doi:10.1029/2010RG000349, 2011.
- Donlon, C., Robinson, I., Casey, K., Vasquez, J., Armstrong, E., Gentemann, C., May, D., LeBorgne, P., Piolle, J., Barton, I., Beggs, H., Poulter, D. J. S., Merchant, C. J., Bingham, A., Heinz, S., Harris, A., Wick, G., Emery, B., Stuart-Menteth, A., Minnett, P., Evans, B., Llewellyn-Jones, D., Mutlow, C., Reynolds, R., Kawamura, H., and Rayner, N.: The Global Ocean Data Assimilation Experiment (GODAE) High Resolution Sea Surface Temperature Pilot Project (GHRSSST-PP), *B. Am. Meteorol. Soc.*, 88, 1197–1213, 2007.
- Evans, M. S. C., Campbell, S. W., Bhethanabotla, V., and Poor, N. D.: Effect of sea salt and calcium carbonate interactions with nitric acid on the direct dry deposition of nitrogen to Tampa Bay, Florida, *Atmos. Environ.*, 38, 4847–4858, 2004.
- Fountoukis, C. and Nenes, A.: ISORROPIA II: a computationally efficient thermodynamic equilibrium model for K^+ – Ca^{2+} – Mg^{2+} – NH_4^+ – Na^+ – SO_4^{2-} – NO_3^- – Cl^- – H_2O aerosols, *Atmos. Chem. Phys.*, 7, 4639–4659, doi:10.5194/acp-7-4639-2007, 2007.
- Fuentes, E., Coe, H., Green, D., de Leeuw, G., and McFiggans, G.: On the impacts of phytoplankton-derived organic matter on the properties of the primary marine aerosol – Part 1: Source fluxes, *Atmos. Chem. Phys.*, 10, 9295–9317, doi:10.5194/acp-10-9295-2010, 2010.
- Gan, C.-M., Binkowski, F., Pleim, J., Xing, J., Wong, D., Mathur, R., and Gilliam, R.: Assessment of the Aerosol Optics Component of the Coupled WRF-CMAQ Model using CARES Field Campaign data and a Single Column Model, *Atmospheric Environment, Atmos. Environ.*, 115, 670–682, doi:10.1016/j.atmosenv.2014.11.028, 2014.
- Gantt, B., Meskhidze, N., and Carlton, A. G.: The contribution of marine organics to the air quality of the western United States, *Atmos. Chem. Phys.*, 10, 7415–7423, doi:10.5194/acp-10-7415-2010, 2010.
- Gard, E. E., Kleeman, M. J., Gross, D. S., Hughes, L. S., Allen, J. O., Morrical, B. D., Fergenson, D. P., Dienes, T., Galli, M. E., Johnson, R. J., Cass, G. R., and Prather, K. A.: Direct observation of heterogeneous chemistry in the atmosphere, *Science*, 279, 1184–1187, 1998.
- Gong, S. L.: A parameterization of sea-salt aerosol source function for sub- and super-micron particles, *Global Biogeochem. Cy.*, 17, 1097, doi:10.1029/2003gb002079, 2003.
- Grythe, H., Ström, J., Krejci, R., Quinn, P., and Stohl, A.: A review of sea-spray aerosol source functions using a large global set of sea salt aerosol concentration measurements, *Atmos. Chem. Phys.*, 14, 1277–1297, doi:10.5194/acp-14-1277-2014, 2014.
- Henderson, B. H., Akhtar, F., Pye, H. O. T., Napelenok, S. L., and Hutzell, W. T.: A database and tool for boundary conditions for regional air quality modeling: description and evaluation, *Geosci. Model Dev.*, 7, 339–360, doi:10.5194/gmd-7-339-2014, 2014.
- Hopkins, R. J., Desyaterik, Y., Tivanski, A. V., Zaveri, R. A., Berkowitz, C. M., Tylliszczak, T., Gilles, M. K., and Laskin, A.: Chemical speciation of sulfur in marine cloud droplets and particles: Analysis of individual particles from the marine boundary layer over the California current, *J. Geophys. Res.*, 113, D04209, doi:10.1029/2007JD008954, 2008.
- Im, U.: Impact of sea-salt emissions on the model performance and aerosol chemical composition and deposition in the East Mediterranean coastal regions, *Atmos. Environ.*, 75, 329–340, doi:10.1016/j.atmosenv.2013.04.034, 2013.
- Jaeglé, L., Quinn, P. K., Bates, T. S., Alexander, B., and Lin, J.-T.: Global distribution of sea salt aerosols: new constraints from in situ and remote sensing observations, *Atmos. Chem. Phys.*, 11, 3137–3157, doi:10.5194/acp-11-3137-2011, 2011.
- Keene, W. C., Maring, H., Maben, J. R., Kieber, D. J., Pszenny, A. A. P., Dahl, E. E., Izaguirre, M. A., Davis, A. J., Long, M. S., Zhou, X. L., Smoydzin, L., and Sander, R.: Chemical and physical characteristics of nascent aerosols produced by bursting bubbles at a model air-sea interface, *J. Geophys. Res.*, 112, D21202, doi:10.1029/2007JD008464, 2007.
- Kelly, J. T., Bhawe, P. V., Nolte, C. G., Shankar, U., and Foley, K. M.: Simulating emission and chemical evolution of coarse sea-salt particles in the Community Multiscale Air Quality (CMAQ) model, *Geosci. Model Dev.*, 3, 257–273, doi:10.5194/gmd-3-257-2010, 2010.
- Kelly, J. T., Baker, K. R., Nowak, J. B., Murphy, J. G., Markovic, M. Z., VandenBoer, T. C., Ellis, R. A., Neuman, J. A., Weber, R. J., Roberts, J. M., Veres, P. R., de Gouw, J. A., Beaver, M. R., Newman, S., and Misenis, C.: Fine-scale simulation of ammonium and nitrate over the South Coast Air Basin and San Joaquin Valley of California during CalNex-2010, *J. Geophys. Res. Atmos.*, 119, 3600–3614, doi:10.1002/2013JD021290, 2014.
- Lewis, E. R. and Schwartz, S. E.: Sea-Salt Aerosol Production: Mechanisms, Methods, Measurements, and Models – A Critical Review, American Geophysical Union, Washington, DC, 2004.
- Long, M. S., Keene, W. C., Easter, R. C., Sander, R., Liu, X., Kerkweg, A., and Erickson, D.: Sensitivity of tropospheric chemical composition to halogen-radical chemistry using a fully coupled size-resolved multiphase chemistry–global climate system: halogen distributions, aerosol composition, and sensitivity of climate-relevant gases, *Atmos. Chem. Phys.*, 14, 3397–3425, doi:10.5194/acp-14-3397-2014, 2014.
- Mårtensson, E. M., Nilsson, E. D., de Leeuw, G., Cohen, L. H., and Hansson, H. C.: Laboratory simulations are parameterization of the primary marine aerosol production, *J. Geophys. Res.*, 108, 4297, doi:10.1029/2002JD002263, 2003.
- McInnes, L. M., Covert, D. S., Quinn, P. K., and Germani, M. S.: Measurements of chloride depletion and sulfur enrichment in individual sea-salt particles collected from the remote marine boundary-layer, *J. Geophys.*, 99, 8257–8268, 1994.
- Monahan, E. C., Spiel, D. E., and Davidson, K. L.: A model of marine aerosol generation via whitecaps and wave disruption, *Oceanic Whitecaps and Their Role in Air-Sea Exchange Processes*, edited by: Monahan, E. C., G. MacNiocaill, Reidel, Dordrecht, the Netherlands, 167–174, 1986.

- Murphy, D., Anderson, J., Quinn, P., McInnes, L., Brechtel, F., Kreidenweis, S., Middlebrook, A., Posfai, M., Thomson, D., and Buseck, P.: Influence of sea-salt on aerosol radiative properties in the Southern Ocean marine boundary layer, *Nature*, 392, 62–65, doi:10.1038/32138, 1998.
- Nolte, C. G., Bhave, P. V., Arnold, J. R., Dennis, R. L., Zhang, K. M., and Wexler, A. S.: Modeling urban and regional aerosols – Application of the CMAQ-UCD Aerosol Model to Tampa, a coastal urban site, *Atmos. Environ.*, 42, 3179–3191, 2008.
- Nolte, C. G., Appel, K. W., Kelly, J. T., Bhave, P. V., Fahey, K. M., Collett Jr., J. L., Zhang, L., and Young, J. O.: Evaluation of the Community Multiscale Air Quality (CMAQ) model v5.0 against size-resolved measurements of inorganic particle composition across sites in North America, *Geosci. Model Dev.*, 8, 2877–2892, doi:10.5194/gmd-8-2877-2015, 2015.
- Norris, S. J., Brooks, I. M., de Leeuw, G., Smith, M. H., Moerman, M., and Lingard, J. J. N.: Eddy covariance measurements of sea spray particles over the Atlantic Ocean, *Atmos. Chem. Phys.*, 8, 555–563, doi:10.5194/acp-8-555-2008, 2008.
- Nowak, J. B., Neuman, J., Bahreini, R., Middlebrook, A. M., Holloway, J., McKeen, S., Parrish, D., Ryerson, T., and Trainer, M.: Ammonia sources in the California South Coast Air Basin and their impact on ammonium nitrate formation, *Geophys. Res. Lett.*, 39, L07804, doi:10.1029/2012GL051197, 2012.
- O’Dowd, C. D., Smith, M. H., Consterdine, I. E., and Lowe, J. A.: Marine aerosol, sea-salt, and the marine sulphur cycle: A short review, *Atmos. Environ.*, 31, 73–80, 1997.
- Ovadnevaite, J., Manders, A., de Leeuw, G., Ceburnis, D., Monahan, C., Partanen, A.-I., Korhonen, H., and O’Dowd, C. D.: A sea spray aerosol flux parameterization encapsulating wave state, *Atmos. Chem. Phys.*, 14, 1837–1852, doi:10.5194/acp-14-1837-2014, 2014.
- Petelski, T. and Chomka, M.: Marine aerosol fluxes in the coastal zone—BAEX experimental data, *Oceanologia*, 38, 469–484, 1996.
- Pierce, J. and Adams, P. J.: Global evaluation of CCN formation by direct emission of sea salt and growth of ultrafine sea salt, *J. Geophys. Res.*, 111, D06203, doi:10.1029/2005JD006186, 2006.
- Riedel, T. P., Wolfe, G. M., Danas, K. T., Gilman, J. B., Kuster, W. C., Bon, D. M., Vlasenko, A., Li, S.-M., Williams, E. J., Lerner, B. M., Veres, P. R., Roberts, J. M., Holloway, J. S., Lefter, B., Brown, S. S., and Thornton, J. A.: An MCM modeling study of nitryl chloride (ClNO₂) impacts on oxidation, ozone production and nitrogen oxide partitioning in polluted continental outflow, *Atmos. Chem. Phys.*, 14, 3789–3800, doi:10.5194/acp-14-3789-2014, 2014.
- Ryerson, T. B., Andrews, A. E., Angevine, W. M., Bates, T. S., Brock, C. A., Cairns, B., Cohen, R. C., Cooper, O. R., de Gouw, J. A., Fehsenfeld, F. C., Ferrare, R. A., Fischer, M. L., Flagan, R. C., Goldstein, A. H., Hair, J. W., Hardesty, R. M., Hostetler, C. A., Jimenez, J. L., Langford, A. O., McCauley, E., McKeen, S. A., Molina, L. T., Nenes, A., Oltmans, S. J., Parrish, D. D., Pederson, J. R., Pierce, R. B., Prather, K., Quinn, P. K., Seinfeld, J. H., Senff, C. J., Sorooshian, A., Stutz, J., Surratt, J. D., Trainer, M., Volkamer, R., Williams, E. J., and Wofsy, S. C.: The 2010 California Research at the Nexus of Air Quality and Climate Change (CalNex) field study, *J. Geophys. Res.*, 118, 5830–5866, doi:10.1002/jgrd.50331, 2013.
- Sarwar, G., Simon, H., Bhave, P., and Yarwood, G.: Examining the impact of heterogeneous nitryl chloride production on air quality across the United States, *Atmos. Chem. Phys.*, 12, 6455–6473, doi:10.5194/acp-12-6455-2012, 2012.
- Sellegri, K., O’Dowd, C. D., Yoon, Y. J., Jennings, S. G., and de Leeuw, G.: Surfactants and submicron sea spray generation, *J. Geophys. Res.-Atmos.*, 111, D22215, doi:10.1029/2005JD006658, 2006.
- Simon, H., Kimura, Y., McGaughey, G., Allen, D. T., Brown, S. S., Osthoff, H. D., Roberts, J. M., Byun, D., and Lee, D.: Modeling the impact of ClNO₂ on ozone formation in the Houston area, *J. Geophys. Res.*, 114, D00F03, doi:10.1029/2008JD010732, 2009.
- Skamarock, W. C., Klemp, J. B., Dudhia, J., Gill, D. O., Barker, D. M., Duda, M. G., Huang, X., Wang, W., and Powers, J. G.: A description of the Advanced Research WRF version 3., NCAR Technical Note NCAR/TN-475+STR, 2008.
- Sofiev, M., Soares, J., Prank, M., de Leeuw, G., and Kukkonen, J.: A regional-to-global model of emission and transport of sea salt particles in the atmosphere, *J. Geophys. Res.*, 116, D21302, doi:10.1029/2010JD014713, 2011.
- Spada, M., Jorba, O., Pérez García-Pando, C., Janjic, Z., and Baldasano, J. M.: Modeling and evaluation of the global sea-salt aerosol distribution: sensitivity to size-resolved and sea-surface temperature dependent emission schemes, *Atmos. Chem. Phys.*, 13, 11735–11755, doi:10.5194/acp-13-11735-2013, 2013.
- Sullivan, R. C. and Prather, K. A.: Investigations of the diurnal cycle and mixing state of oxalic acid in individual particles in Asian aerosol outflow, *Environ. Sci. Technol.*, 41, 8062–8069, 2007.
- Tang, I. N., Tridico, A. C., and Fung, K. H.: Thermodynamic and optical properties of sea salt aerosols, *J. Geophys. Res.*, 102, 23269–23275, 1997.
- Tyree, C. A., Hellion, V. M., Alexandrova, O. A., and Allen, J. O.: Foam droplets generated from natural and artificial seawaters, *J. Geophys. Res.*, 112, D12204, doi:10.1029/2006JD007729, 2007.
- Vignati, E., de Leeuw, G., and Berkowicz, R.: Modeling coastal aerosol transport and effects of surf-produced aerosols on processes in the marine atmospheric boundary layer, *J. Geophys. Res.-Atmos.*, 106, 20225–20238, 2001.
- Weber, R. J., Orsini, D., Daun, Y., Lee, Y. N., Klotz, P. J., and Brechtel, F.: A Particle-into-Liquid Collector for Rapid Measurement of Aerosol Bulk Chemical Composition, *Aerosol Sci. Technol.*, 35, 718–727, doi:10.1080/02786820152546761, 2001.
- White, W. H.: Chemical markers for sea salt in IMPROVE aerosol data, *Atmos. Environ.*, 42, 261–274, 2008.
- Yang, X., Cox, R., Warwick, N., Pyle, J., Carver, G., O’Connor, F., and Savage, N.: Tropospheric bromine chemistry and its impacts on ozone: A model study, *J. Geophys. Res.*, 110, D23311, doi:10.1029/2005JD006244, 2005.
- Zábori, J., Matisans, M., Krejci, R., Nilsson, E. D., and Ström, J.: Artificial primary marine aerosol production: a laboratory study with varying water temperature, salinity, and succinic acid concentration, *Atmos. Chem. Phys.*, 12, 10709–10724, doi:10.5194/acp-12-10709-2012, 2012a.
- Zábori, J., Krejci, R., Ekman, A. M. L., Mårtensson, E. M., Ström, J., de Leeuw, G., and Nilsson, E. D.: Wintertime Arctic Ocean sea water properties and primary marine aerosol concentrations, *Atmos. Chem. Phys.*, 12, 10405–10421, doi:10.5194/acp-12-10405-2012, 2012b.

Zhang, K. M., Knipping, E. M., Wexler, A. S., Bhave, P. V., and Tonnesen, G. S.: Size distribution of sea-salt emissions as a function of relative humidity, *Atmos. Environ.*, 39, 3373–3379, 2005.

Zhang, K. M., Knipping, M. E., Wexler, A. S., Bhave, P. V., and Tonnesen, S. G.: Reply to comment on “Size distribution of sea-salt emissions as a function of relative humidity”, *Atmos. Environ.*, 40, 591–592, 2006.